REMONTEE BOUEUSE ET CREATION DE LA COUCHE INTERMEDIAIRE DANS LA SOUS-STRUCTURE FERROVIAIRE

MUD PUMPING AND INTERLAYER CREATION IN RAILWAY SUB-STRUCTURE

Trong Vinh DUONG[1], Yu-Jun CUI[1], Anh Minh TANG[1], Nicolas CALON[2], Alain ROBINET[2], Jean-Claude DUPLA[1],

[1]: Ecole des Ponts ParisTech, U.R. Navier/CERMES
[2]: French railway company (SNCF)

RÉSUMÉ – Les facteurs principaux pour la création de la couche intermédiaire et la remontée boueuse dans la sous-structure ferroviaire sont étudiés via des modèles physiques. Il apparaît qu'à faible densité de sol, la dissipation de la pression d'eau entraine la remontée boueuse, alors qu'à forte densité, la migration des fines engendrée par la pénétration du ballast dans le sol support, crée la couche intermédiaire.

ABSTRACT –The driving factors for the interlayer creation and mud pumping phenomena in railway sub-structure was investigated through physical modelling. It appears that in case of low soil density, the dissipation of pore water pressure in the sub-soil gave rise to mud pumping. But in In case of higher soil density, the upward migration of fine particles was generated by the penetration of ballast into the sub-soil, forming the interlayer.

1. Introduction

Railway track-bed must be regularly maintained. To optimize the maintenance should be optimized, it is essential to well understand the degradation process of track-bed. In France, during the maintenance campaign of the conventional tracks, a new layer namely interlayer was identified. It is suspected that this layer was formed mainly by the interpenetration between ballast and sub-soil. It has been found that this interlayer can play an important role in the overall behavior of railway tracks (Trinh et al., 2011; Trinh, 2011; Trinh et al., 2012; Cui et al., 2013; Duong et al., 2013). On the other hand, the mud pumping which is characterized by the fast upward migration of sub-soil fine particles through the ballast voids has been known to be the worst degradation phenomenon for the railway sub-structure. This phenomenon was reported by several authors in the field of railway sub-structure (Ayres, 1986; Selig and Waters, 1994; Raymond, 1999; Sussmann et al., 2001; Burns et al., 2006; Gataora et al., 2006; Aw 2007; Indraratna et al., 2011). Basically, these two phenomena (interlayer creation and mud pumping) are both related to the migration of fine particles and the interaction between ballast and sub-soil layers. Thus, a good knowledge on the mechanism related to the migration of fine particles is crucial for better understanding the interlayer creation and the mud-pumping, and also for further proposing efficient and economic methods for railway track maintenance.

To date, even though the migration of fine particles and its consequence has been reported in several studies, the knowledge on the driving mechanism of this phenomenon remains scarce. For the interlayer, as it has been recently recognized, the question about its creation is still completely open. For the mud pumping, several mechanisms were proposed but they are sometimes contradictory: Takatoshi (1997) proposed that the mud pumping is due to the suction generated by the upward and downward moving of ties. On

the contrary, Alobaidi and Hoare (1996; 1999) proposed that this phenomenon is mainly due to the water pressure developed at the interface between the sub-grade and sub-base or ballast layers. Van (1985) proposed some models for describing the mud pumping in the pavement context but their application in the railway context remains to be verified based on relevant experimental data.

In the present work, using a transparent apparatus recently developed, the mechanisms of mud pumping and interlayer creation in conventional railway tracks were investigated. The results obtained allowed the driving factors for the mud pumping and interlayer creation phenomena to be analyzed.

2. Materials and methods

The sub-soil used in this study was prepared from crushed sand and kaolin (70%/30% by dry mass), namely*70S30K*. The reason of using this artificial material is that it can be reproduced easily in the laboratory for having a large quantity required for the whole test program, thus avoiding any problems related to the natural soil heterogeneity – the composition of soil can be slightly different from one sample to another. The material used in this study has a high percentage of fines (the particles smaller than 80 µm represent 95%), similar to the sub-soils found at the sites with mud pumping identified (Alobaidi and Hoare, 1996; Aw, 2007). The mixture also has a grain size distribution curve similar to that of a widely studied soil - the Jossigny silt (Fleureau and Indarto, 1995; Cui and Delage, 1996). Figure 1 shows the grain size distribution curves of the materials used, along with the curve of Jossigny silt.

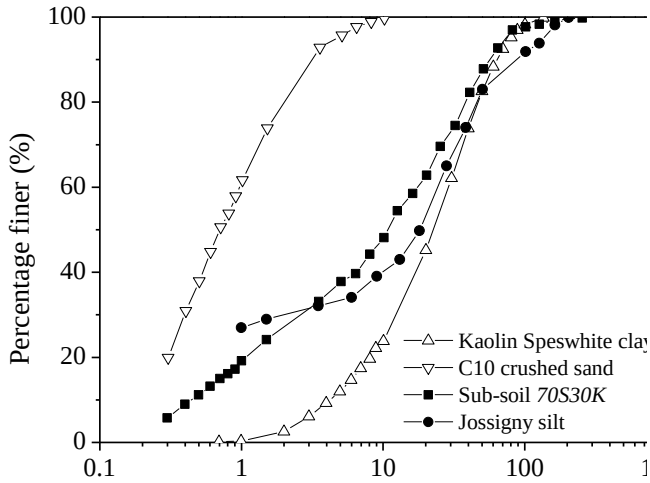

Figure 1: Grain size distribution curve of the studied materials

Some other characteristics of the studied sub-soil are presented in Tableau 1. Standard proctor test showed that *70S30K* has an optimum water content of 16% and a maximum dry unit mass of 1.78 Mg/m^3. The ballast used was taken from the storage of construction materials of the French Railways Company (SNCF) and its characteristics meet the corresponding standard of SNCF.

Tableau 1: Characteristics of sub-soil 70S30K

Unit mass of clay particles ρ_s	2.60
Unit mass of crushed sand ρ_s	2.65
Liquid Limit w_L	27%
Plasticity Index Ip	11%
Optimum water content w	16%

Figure 2 presents a schematic view of the 1G physical model, with a 3D view (Figure 2a), a side view (Figure 2b) and a view of cross section A-A (Figure 2c). The cylindrical cell has an internal diameter of 550 mm, a wall thickness of 20 mm and a height of 600 mm. The wall was made of Poly(methyl methacrylate) - PMMA which is a transparent thermoplastic allowing the observation of sample from outside. The following devices were installed: a digital camera connected to a computer, that allows the visual monitoring of the ballast/sub-soil interface; a LED series installed on the top of the PMMA wall, lighting up the apparatus wall and improving the visual monitoring conditions by the digital camera; three time-domain refectory probes (TDR1 to TDR3) embedded in the sub-soil (*h* = 120, 160, 200 mm), that allow the volumetric water content to be monitored; three tensiometers (T1 to T3) installed in couple with TDRs at different heights (*h* = 120, 160, 200 mm). They were home-made with the same principle as that for high capacity tensiometer (Ridley et al., 2003; Mantho 2005, Cui et al., 2008; Toll et al., 2012; Lourenço et al., 2011). One pressure sensor installed at the bottom of the apparatus (*h* = 0 mm) for measuring the positive pore water pressure under saturated conditions. A hydraulic actuator with the integrated displacement and force sensors, that allows monotonic or cyclic loadings.

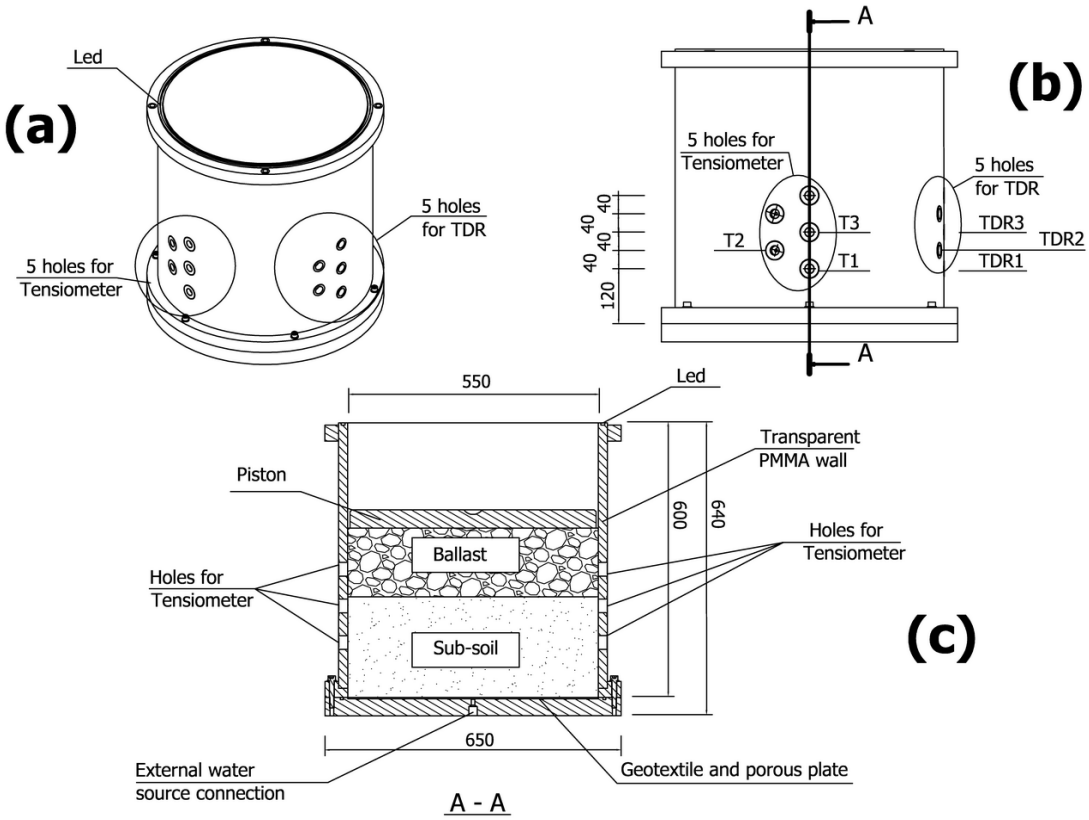

Figure 2: Schematic view of the apparatus developed

For the soil specimen preparation, water was added to *70S30K* to reach the optimum water content *w* = 16 %. The soil specimen was then prepared by manual compaction in five layers of 40 mm thick each and one layer of 20 mm thick, making a total of 220 mm thickness for the whole specimen. For the dry unit mass, three values were considered: 1.4, 1.5 and 1.6 Mg/m^3. These values are close to those considered by other authors: 1.45 Mg/m^3 by Burns et al. (2006) and from 1.52 to 1.54 Mg/m^3 by Alobaidi et al. (1999). According to Burns et al. (2006), the values in this range correspond to the medium strength field conditions. The TDR probes were placed between the compaction layers. A

160 mm ballast layer was placed on the sub-soil and the surface of ballast layer was arranged in order to be horizontal for ensuring a good ballast/piston contact. The whole apparatus was put under the hydraulic actuator. Finally, the tensiometers were installed and other devices were set on (lighting up the LED series, setting up the camera).

Three tests were conducted with three values of initial dry unit mass: 1.4 (E1), 1.5 (E2) and 1.6 Mg/m^3 (E3). All the tests started with the sub-soil in unsaturated state (w = 16 %) and with a pre-loading stage: monotonic loading from 0 to 100 kPa at a rate of 2 kN/min; low-frequency cyclic loading from 30 to 100 kPa; 0.1 Hz cyclic loading for 20 cycles; 1 Hz cyclic loading for 50 cycles and 2 Hz cyclic loading for 100 cycles. Afterwards, a 5 Hz cyclic loading for 500 000 cycles was applied. The value of 5 Hz frequency represents the train circulation at 100 km/h and the applied stress was chosen according to the stress distribution in the conventional railway tracks in France (Trinh, 2011).

In order to study the effect of water content or degree of saturation, once the 500 000 cycles ended, the sub-soil was saturated from the bottom under a hydraulic head of 12 kPa. After saturation, the water level was maintained at 20 mm above the ballast/sub-soil interface in order to ensure the saturated state of the sub-soil. Before the loading under saturated condition, a pressure sensor was installed at h = 0 mm. Monotonic loading at the same rate as in the unsaturated case was then applied followed by the 5 Hz cyclic loading. The test ended when fine particles were observed on the surface of the ballast layer or when the number of cycles reached 500 000.

3. Results

Figure 3 depicts the evolutions of permanent displacement during the 5 Hz loading under the unsaturated condition. The displacement was insignificant during the first 100 cycles. Beyond 100 cycles, it increased almost linearly with the logarithm of number of cycles. This is consistent with the constitutive models for unbound granular behavior reported in Paute and Le Fort (1984); Hornych (1993) and AFNOR (1995). The comparison of the values at the end of cyclic loading (500 000 cycles) shows that the lower the dry unit mass, the larger the permanent axial displacement. The slope change in test E1 was probably due to a problem of the horizontality of piston.

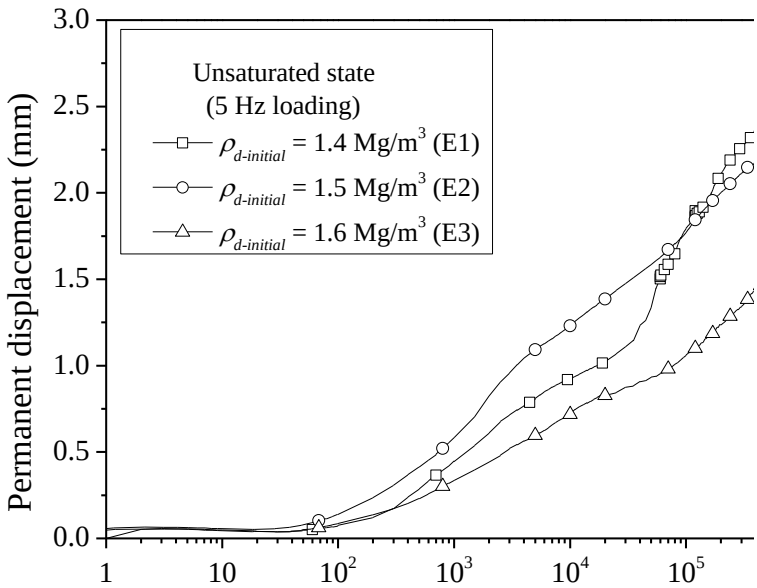

Figure 3: Permanent displacement during 5 Hz loading (w = 16%)

Figure 4 depicts the evolutions of volumetric water content of sub-soil from the beginning of the test to the end of the 5 Hz loading for 500 000 cycles. After compaction, with the same initial water content w = 16%, as expected, the average volumetric water content (θ) increased with dry unit mass. During the pre-loading stage, there was an increasing trend at all levels and in all tests. The increase of θ at h = 200 mm (20 mm below the ballast/sub-soil surface) was the most pronounced. This can be explained by the ballast penetration into the sub-soil and the settlement of sub-soil that can result in a decrease of sub-soil void, thereby increasing the volumetric water content. During the 5 Hz loading for 500 000 cycles, the water content was stable.

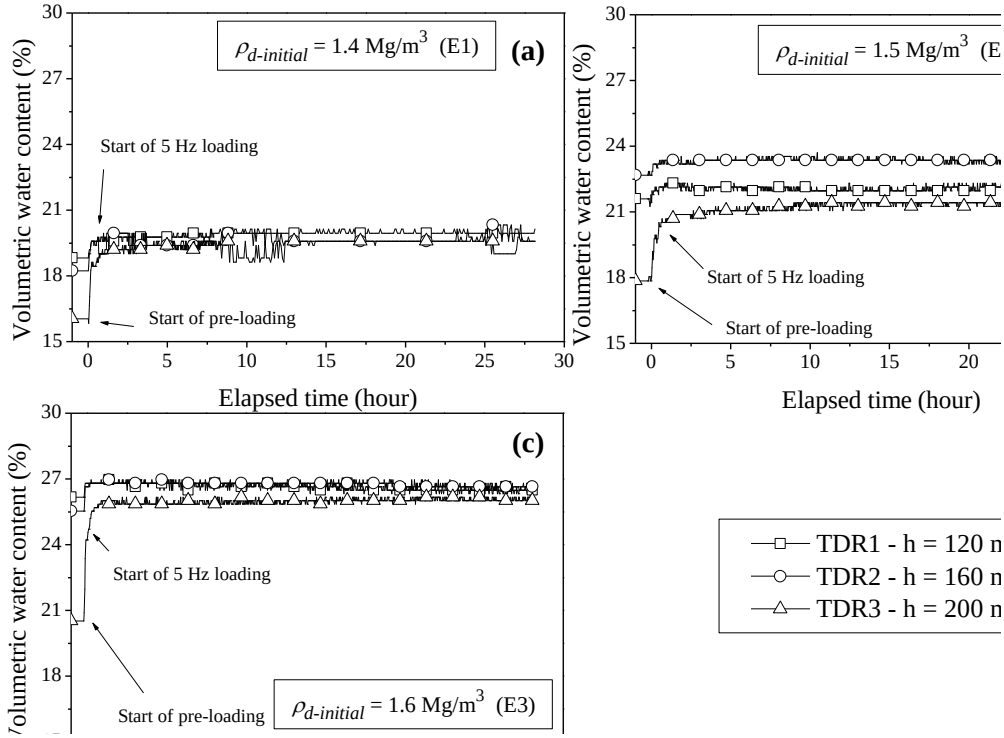

Figure 4: Evolutions of volumetric water content for 500 000 cycles at 5 Hz

When the 5 Hz loading for 500 000 cycles in the unsaturated state ended, the sub-soil was saturated. A typical result of variations of volumetric water content from test E2 during saturation is presented in Figure 5a. The corresponding increase of pore water pressure (or suction decrease) is presented in Figure 5b. The three levels show the same variations, suggesting a quite fast water flow through the sample. It took about 20 hours for the volumetric water content to reach stabilization, while about 60 hours were required for the pore water pressure to reach zero. In addition, when the volumetric water content became steady, the pore pressure continued increasing. It is well known that during the saturation of fine-grained soils, it is very difficult to reach S_r = 100% and the hydraulic permeability of clayey soils is relatively low (Romeo 2013). During saturation, the macro-pores are filled first, while it takes longtime for water to fill the micro-pores. This can be observed also in Figure 5b. The fact that the evolutions of the pore water pressures at all three levels are the same confirms that the micro-pores were filled quickly and the suction changes were governed mainly by the micro-pores filling process. At the end of saturation stage where water level was fixed at 2 mm above the ballast/sub-soil interface, the water pressures given by the tensiometers were consistent with the hydraulic levels: a higher water pressure was obtained at a lower hydraulic level. This partly indicates the good performance of the tensiometers used.

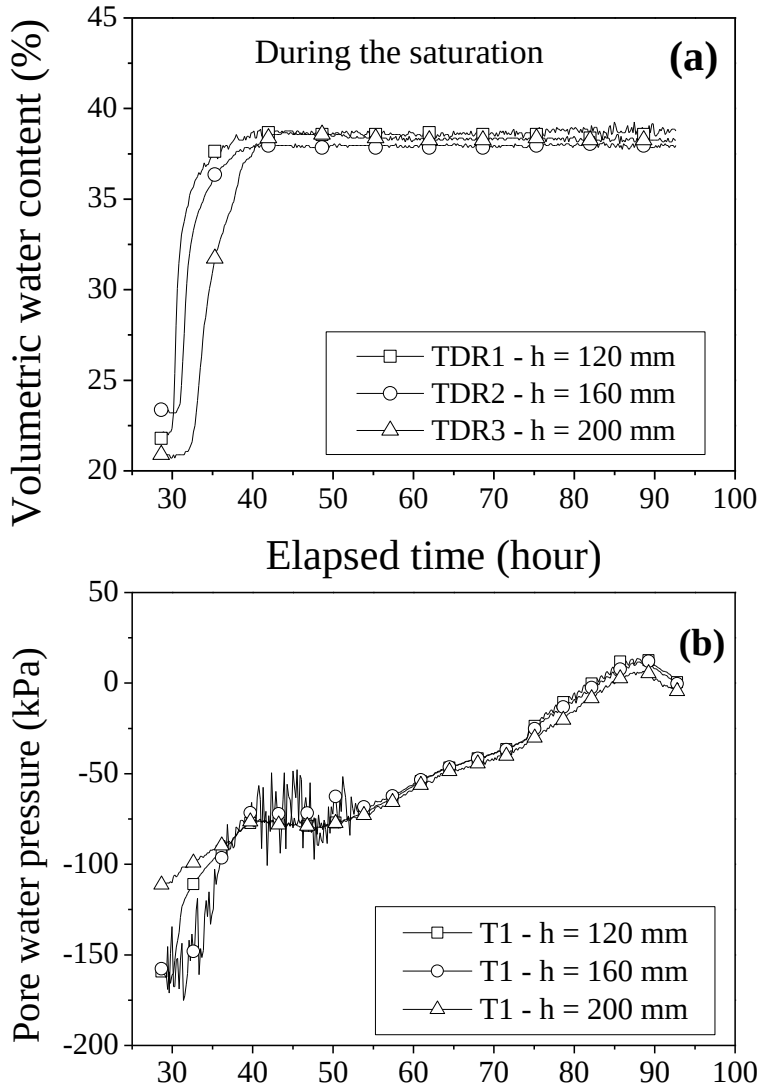

Figure 5: Typical result of volumetric water content and pore water pressure during the saturation of sub-soil ($\rho_{d\text{-initial}}$ = 1.5 Mg/m^3)

At the end of saturation stage, loadings were applied again. Figure 6 shows the evolution of interface in test E1. The photographs were taken at three moments: before loading in the saturated state, after the monotonic loading and after the cyclic loading. They are presented in Figure 6a, b, c, respectively. It can be seen clearly that fine particles were pumped up as loadings were applied.

Figure 7 presents the photographs of test E2 taken at the ballast/sub-soil interface at three moments (after the saturation, after the monotonic loading and after the cyclic loading). As in the previous case, the fine particles were pumped up significantly especially during the cyclic loading.

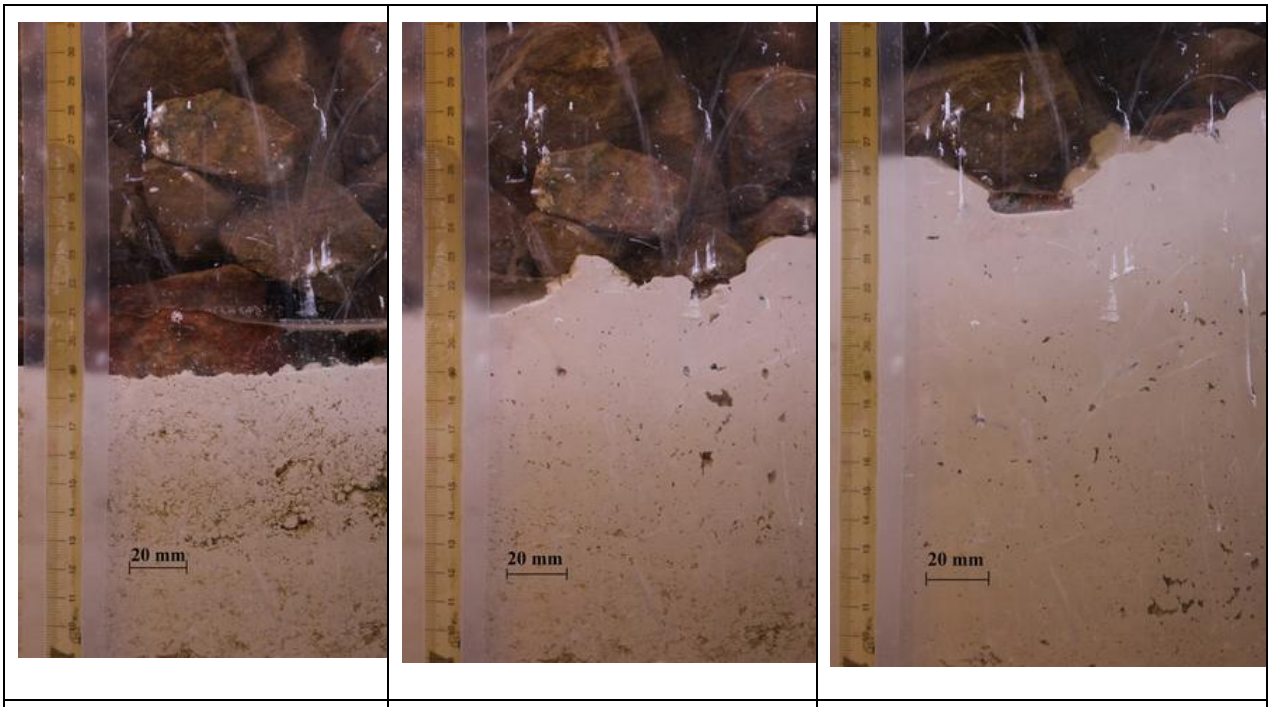

a) After saturation and before monotonic loading	b) After monotonic loading (saturated state)	c) After cyclic loading (saturated state)

Figure 6: Photographs showing the evolution of the ballast/sub-soil interface ($\rho_{d\text{-initial}}$ = 1.4 Mg/m^3).

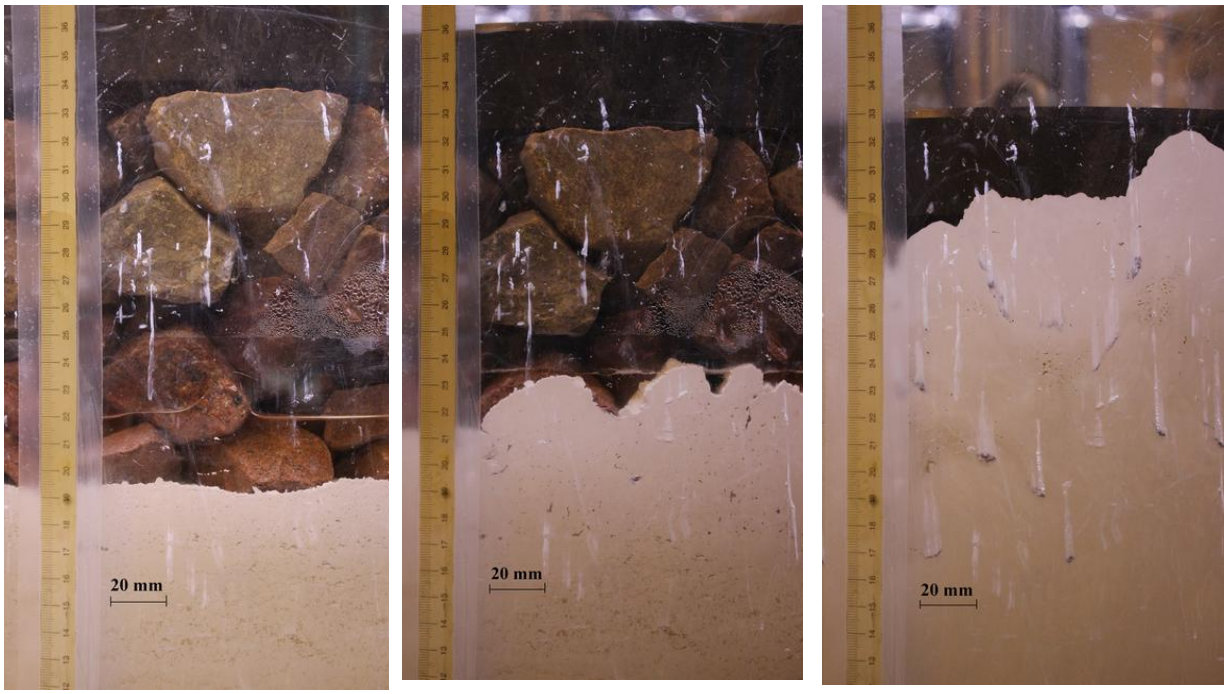

a) After saturation and before monotonic loading

b) After monotonic loading (saturated state)

c) After cyclic loading (saturated state)

Figure 2: Photographs showing the evolution of the ballast/sub-soil interface: ($\rho_{d\text{-initial}}$ = 1.5 Mg/m^3).

Figure 8 shows the photographs taken in test E3 right before the monotonic loading (Figure 8a), after the monotonic loading (Figure 8b) and after the cyclic loading (Figure 8c). The movement of fine particles can be also observed. During the monotonic loading, fine particles moved up, but much less than in the previous tests. Even after a large number of cycles, the sub-soil level rose up by about 20 mm, and there was no fine particles pumped up to the ballast surface.

a) After saturation and before monotonic loading

b) After monotonic loading (saturated state)

c) After cyclic loading (saturated state)

Figure 8: Photographs showing the evolution of the ballast/sub-soil interface ($\rho_{d\text{-initial}}$ = 1.6 Mg/m^3).

4. Conclusions

Using a 1G physical model developed, the mud pumping and the interlayer creation phenomena in the context of railway sub-structure were studied by investigating the driving factors. The soil sample was prepared in two layers, one ballast layer overlying one sub-soil layer, representing the conventional railway sub-structure in France. The tests were conducted at two water contents and three densities of sub-soil with monotonic and cyclic loadings.

The analysis of the ballast settlement through the particles movement, the global displacement and the sub-soil settlement showed that the sub-soil state can strongly influence the ballast behavior: the larger the initial dry unit mass of sub-soil, the lower the permanent axial displacement. This suggests that in order to understand the overall behavior of railway sub-structure, it is important to take into account the interaction between the different layers involved.

The presence of water was found to be the most crucial factor for the migration of fine particles. In the unsaturated state, both the ballast and sub-soil settlements occurred, but without the migration of fine particles. Under the near saturated state, the ballast/sub-surface interface moved up, and the pumping level depends on the sub-soil dry unit mass. In the case of $\rho_{d\text{-initial}}$ = 1.4 Mg/m^3 and 1.5 Mg/m^3, under the cyclic loadings, the pore water

pressure was higher than the minimum value of applied stress, resulting in sub-soil liquefaction. Excess pore water pressure dissipation took place, bringing fine particles upward. This corresponds to the mud pumping phenomenon. In the case of $\rho_{d\text{-}initial}$ = 1.6 Mg/m^3, there was just the interpenetration of ballast and sub-soil, resulting in a mixture layer namely interlayer.

5. References

AFNOR. 1995. NF P98-235-1: Essais relatif aux chaussées. Matériaux non traitées. Part 1: Essai triaxial à chargements répétés*. French Standard*, (In French).

Alobaidi, I., Hoare, D.J., 1994. Factors affecting the pumping of fines at the subgrade-subbase interface of highway pavements: A laboratory study. *Geosynthetics International* 1 (2), 221–259.

Alobaidi, I., Hoare, D.J., 1996. The development of pore water pressure at the subgrade-subbase interface of a highway pavement and its effect on pumping of fines. *Geotextiles and Geomembranes* 14 (2), 111–135.

Alobaidi, I., Hoare, D.J., 1999. Mechanisms of pumping at the subgrade-subbase interface of highway pavements. *Geosynthetics International* 6 (4), 241–259.

Aw, E.S., 2007. Low cost monitoring system to diagnose problematic rail bed: Case study at mud pumping site. *PhD Dissertation*, Massachusetts Institute of Technology, USA.

Ayres, D.J., 1986. Geotextiles or geomembranes in track? British railway experience. *Geotextiles and Geomembranes* 3 (2-3), 129–142.

Burns, B., Ghataora, G.S., Sharley, P., 2006. Development and testing of geosand composite layers using a pumping index test. In Proceedings of the First International *Conference on Railway Foundations Railfound06*, University of Birmingham, UK, 385–393.

Cui, Y.J., Delage, P., 1996. Yielding behaviour of an unsaturated compacted silt. *Géotechnique* 46 (2), 291-311.

Cui, Y.J., Tang, A.M., Loiseau, C., Delage, P., 2008. Determining the unsaturated hydraulic conductivity of a compacted sand-bentonite mixture under constant-volume and free-swell conditions. *Physics and Chemistry of the Earth*, Parts A/B/C, 33, S462–S471.

Cui, Y.J., Duong, T.V., Tang, A.M., Dupla, J., Calon, N., Robinet, A., 2013. Investigation of the hydro-mechanical behaviour of fouled ballast. *Journal of Zhejiang University-Science A* 14 (4), 244-255.

Duong, T.V., Trinh, V.N., Cui, Y.J., Tang, A.M., Nicolas, C., 2013. Development of a large-scale infiltration column for studying the hydraulic conductivity of unsaturated fouled ballast. *Geotechnical Testing Journal* 36 (1), 54-63.

Fleureau, J.M., Indarto, 1995. Comportement du limon de Jossigny remanié soumis à une pression interstitielle négative. *Revue Française de Géotechnique* 62, 59-66. (In French).

Ghataora, G.S., Burns, B., Burrow, M.P.N., Evdorides, H.T., 2006. Development of an index test for assessing anti-pumping materials in railway track foundations. In: *Proceedings of the First International Conference on Railway Foundations, Railfound06*, University of Birmingham, UK, 355–366.

Hornych, P., Corté, J.F., Paute, J.L., 1993. Etude des déformations permanentes sous chargements répétés de trois graves non traitées. *Bulletin de Liaison des Laboratoires des Ponts et Chaussées* 184, 77-84 (In French).

Indraratna, B., Salim, W., Rujikiatkamjorn, C., 2011. *Advanced Rail Geotechnology - Ballasted Track,* CRC Press.

Lourenço, S.D.N., Gallipoli, D. Toll, D.G., Augarde, C.E., Evans, F.D., 2011. A new procedure for the determination of soil-water retention curves by continuous drying using high-suction tensiometers. *Canadian Geotechnical Journal* 48 (2), 327–335.

Mantho, A.T., 2005. Echanges sol-atmosphère application à la sécheresse. *PhD Dissertation, Ecole Nationales des Ponts et Chaussées - Université Paris – Est,* France (In French).

Paute, J.L., Le Fort, R., 1984. Determination of untreated gravels mechanical characteristics with cyclic loading triaxial apparatus. *Bulletin of the International Association of Engineering Geology* (29), 419 – 424, (In French).

Raymond, G.P., 1999. Railway rehabilitation geotextiles. *Geotextiles and Geomembranes* 17 (4), 213–230.

Ridley, A., Dineen, K., Burland, J., Vaughan, P., 2003. Soil matrix suction: some examples of its measurement and application in geotechnical engineering. *Géotechnique* 53 (2), 241-254.

Romeo, E., 2013. A microstructural insight into compacted clayey soils and their hydraulic properties*. Engineering Geology* 165, 3-19.

Selig, E.T., Waters, J.M., 1994. Track Geotechnology and Substructure Management, Thomas Telford.

Sussmann, T., Maser, K., Kutrubes, D., Heyns, F., Selig, E., 2001. Development of ground penetrating radar for railway infrastructure condition detection. *Symposium on the Application of Geophysics to Engineering and Environmental Problems 2001*.

Takatoshi, I., 1997. Measure for stabilization of railway earth structure. *Japan Railway Technical Service,* 290.

Toll, D.G., Lourenço, S.D.N., Mendes, J., 2012. Advances in suction measurements using high suction tensiometers. *Engineering Geology* 165, 29-37.

Trinh, V.N., (2011). Comportement hydromécanique des matériaux constitutifs de plateformes ferroviaires anciennes. *PhD Dissertation, Ecole Nationales des Ponts et Chaussées - Université Paris – Est,* France (In French).

Trinh, V.N., Tang, A.M., Cui, Y.J., Canou, J., Dupla, J., Calon, N., Lambert, L., Robinet, A., Schoen, O., 2011. Caractérisation des matériaux constitutifs de plate-forme ferroviaire ancienne. *Revue Française de Géotechnique* (134-135), 65–74 (In French).

Trinh, V.N., Tang, A.M., Cui, Y.J., Dupla, J., Canou, J., Calon, N., Lambert, L., Robinet, A., Schoen, O., 2012. Mechanical characterisation of the fouled ballast in conventional railway track sub-structure by large-scale triaxial tests. *Soils and Foundations* 52 (3), 511-523.

Van, W.A., 1985. Rigid pavement pumping: (1) subbase erosion and (2) economic modeling: informational report. *Publication FHWA/IN/JHRP-85/10. Joint Highway Research Project, Indiana Department of Transportation and Purdue University, West Lafayette, Indiana, USA*, doi: 10.5703/1288284314094.